ACTA METALLURGICA SLOVACA
2023, VOL. 29, NO. 4, 187-191

RESEARCH PAPER

THE EFFECT OF MIXING METHODS BEFORE THE DECOMPOSITION PROCESS OF FERRONICKEL SLAG

Wahyu Mayangsari [1], Agus Budi Prasetyo [1], Eni Febriana [1], Ahmad Maksum [2], Rudi Subagja [1], Florentinus Firdiyono [1], Johny Wahyuadi Soedarsono [3]*

[1] Research Center for Metallurgy, National Research and Innovation Agency (BRIN), KST B. J. Habibie, Tangerang Selatan, 15314, Indonesia
[2] Department of Mechanical Engineering, Politeknik Negeri Jakarta G.A. Siwabessy street, Kampus Baru UI Depok, 16425, Indonesia,
[3] Prof Johny Wahyuadi Laboratory, Department of Metallurgical and Materials Engineering, Universitas Indonesia, Depok 16424, Indonesia

*Corresponding author: wahy049@brin.go.id, tel.: +6281119333616, Research Center for Metallurgy, National Research and Innovation Agency, Gedung 720, KST BJ Habibie, Serpong, Tangerang Selatan, Banten, 15314, Indonesia

Received: 14.09.2023
Accepted: 03.12.2023

ABSTRACT

Ferronickel slag is the by-product that was obtained from ferronickel production and contains Si and Mg as the main elements. The decomposition process using alkali could decrease energy consumption to process ferronickel slag by decreasing its melting point. The mixing methods before the decomposition process could significantly affect the interaction between reactants over the process, therefore it is essential to study. This study aims to determine the effect of mixing methods of ferronickel slag and NaOH prior decomposition process on the chemical composition, phase, and microstructure of decomposed ferronickel slag. Two different mixing methods, physical mixing and impregnation, followed by roasting process at 350 °C for 60 minutes were performed, characterized, and analysed. Thermodynamic analysis was calculated and shows a good agreement with the characterization results which the formation of sodium silicate, magnesium hydroxide and iron oxide were identified. The formation of spotty decomposition and distribution of the product layer can be observed as the decomposed ferronickel slags that were priorly mixed by physical mixing and impregnation, respectively. Therefore, the effectiveness of impregnation over physical mixing was investigated.

Keywords: ferronickel, slag, decomposition, alkali, mixing, impregnation, physical mixing.

INTRODUCTION

Nickel production in Indonesia has increased sharply as well as globally. Report of USGS shows that nickel production in Indonesia was about 130,000 metric ton in 2015 and dramatically escalated up to 1,600,00 metric ton in 2022, almost half of worldwide nickel total production [1], [2]. Consequently, the by-product, ferronickel slag, increased as well since the production of a part of ferronickel generated 8 - 14 parts of ferronickel slag. Increasing the value added of ferronickel slag could support a circular economy and is essential to tackle further problems that might emerge due to its accumulation and complex chemical content that might be environmentally leached to the soil and ground water. Furthermore, it has various opportunities to recycle [3]. Previous studies were conducted to utilize ferronickel slag as materials for cement [4] – [7], concrete [8]–[11], polymer [12], mortar [7], [8], magnesium [13] – [15], magnesium metal and ferro alloy [16] as well as for refractory [17].

The ferronickel slag contains SiO_2 41 – 46%, MgO 30 – 41%, Fe_2O_3 10 – 14%, Al_2O_3 2 – 5%, Cr_2O_3 1,4 – 1,9% and other compounds including rare earth elements (REE) in the amount of less than 1% [15], [18]. It allows ferronickel slag to be used as secondary raw materials for Si, Mg and REE as well through pyrometallurgy, hydrometallurgy, and combination of both processes. However, refractory components in the ferronickel slag such as SiO_2 and MgO, caused it has high melting point, about 1450 – 1650 ° C. Therefore, high energy is required for ferronickel slag processing. Decomposition process can be performed to reduce high energy that is required for the process. Some processes such as alkali roasting [18], reduction process [16], [19] – [21], leaching [12], [22] – [23], and combination of these processes [14] – [15], [24] – [26] were studied. Na_2CO_3 addition could reduce the melting point of the mixture to about 850 ° C [18], [27]. Utilization of lower melting point chemicals such as Na_2O_2 [26], NaOH, and Na_2SiO_3 [12] allow decomposition process conducted at lower temperature.

Beside the energy consideration, contact between reactants with respect to the mixing process, however, influences characterizations of decomposed product. Solid-solid mixing is a simple method prior to decomposition process, but it needs higher temperature and longer time to decompose as well as smaller particle size to enlarge contact area that also needs additional time for milling and sieving. On the other hand, solid-liquid mixing is expected in resulting better reactions and diffusions processes by using lower energy since diffusion occurred from solid to liquid more quickly and vice – versa. In the leaching process that solid-liquid reaction conducted, contact between reactants can be maximized by various parameters such as solid to liquid ratio and mixing speed. However, in the pyrometallurgical process, such as reduction and roasting, mixing process thoroughly might bring different results since it affects interaction between reactants. Therefore, it is essential to study to determine the appropriate preliminary process, primarily to promote better reactions.

DOI: 10.36547/ams.29.4.1925

In this study, ferronickel slag and NaOH were mixed by two different methods, roasted, and characterized. Transformation of chemical composition, phase, and microstructure of roasted ferronickel slag with two different mixing methods were determined and discussed. This provides a new insight into mixing mechanism in the preliminary step of decomposition process for ferronickel slag using NaOH with lower energy consumption that led sodium silicate formation, and subsequently directed to the selective silica separation and upgrading remaining metals contained.

MATERIAL AND METHODS

Materials

In this study ferronickel slag was obtained from a smelting plant in Morowali, Central Sulawesi, Indonesia. The ferronickel slag was prepared by drying at 110 °C for 12 hours in the oven followed by crushing, milling, and sieving to produce ferronickel slag with particle size of -149 µm. Analytical chemical grade of sodium hydroxide (NaOH) from Merck was previously mixed by both, physical mixing, and impregnation, to decompose the sieved ferronickel slag in the roasting process.

Methods

The sieved ferronickel slag and NaOH were weighted with ratio of 1:1 by weight prior mixing process that was conducted into two methods, physical mixing, and impregnation. For the former, NaOH pellets were directly mixed to the ferronickel slag by physical mixing before roasted at 350 °C for 60 minutes, and the roasted product is mentioned as RWI. For the later, NaOH was diluted in the distilled water before impregnated to the weighted ferronickel slag that accompanied by mixing at 200 rpm and heating at 100 °C. The impregnated mixture was then evaporated at 110 °C for 240 minutes, followed by roasting at 350 °C for 60 minutes, and the roasted product cited as RI. Roasting process of both were conducted in the carbolite furnace CWF 1300 using ceramic crucible and incurred subsequently after reaching ambient temperature. Furthermore, RWI and RI were characterized to determine the effect of mixing methods prior the decomposition process of the ferronickel slag. Thermodynamic analysis was counted by using HSC Chemistry 6.0.

Characterizations

XRF (X-ray fluorescence), XRD (X-ray diffraction), and SEM-EDS (Scanning Electron Microscope-Energy Dispersive Spectroscopy) analysis were conducted to the sieved ferronickel slag, RI and RWI to investigate the transformations. XRF analysis was performed using Bruker S2 Puma to determine chemical compositions. XRD analysis was carried out by Smartlab Rigaku at a 2θ angle from 20 – 80 °, using Cu anode and wavelength of 1.541487A to interpret the phase transformation. Moreover, SEM-EDS was performed by JOEL Jsm 6390A to figure out the morphology transformations, semi-quantitative chemical composition in the specific area, and mapping.

RESULTS AND DISCUSSION

Thermodynamic analysis

Olivine ($(Mg,Fe)_2SiO_4$) is the main phase of ferronickel slag [18], [26], [28], which is in the atmospheric condition sintering of the olivine could be detected as Mg_2SiO_4, SiO_2, Fe_2O_3 [18], [26], Fe_2SiO_4 [14] [15] and $MgSiO_3$ [29] . Based on the main phase in the ferronickel slag, reactions between ferronickel slag and NaOH in the decomposition process are proposed as follows:

$$SiO_2 + 2NaOH \rightarrow Na_2SiO_3 + H_2O \quad (1)$$

$$Fe_2SiO_4 + 2NaOH \rightarrow Na_2SiO_3 + 2FeO + H_2O \quad (2)$$

$$MgSiO_3 + 2NaOH \rightarrow Na_2SiO_3 + Mg(OH)_2 \quad (3)$$

$$Mg_2SiO_4 + 2NaOH \rightarrow Na_2SiO_3 + 2Mg(OH)_2 \quad (4)$$

Fig. 1 shows the graph of Gibbs free energy of ferronickel slag and NaOH for reaction (1) – (4) at temperature of 0 – 1100 ˚ C. Reactions (1) and (2) indicate spontaneous reaction can be occurred over the temperature range. However, the value of Gibbs free energy tends to increase as temperature rise and become unspontaneous for reactions (3) and (4) at temperature of about 900 ˚ C and 620 ˚ C, respectively. It shows that decomposition can be performed at low temperatures and provides beneficial impact for energy utilization. Moreover, formation of product reactions as mentioned in reaction (1) – (4) can be confirmed by XRD analysis in the further discussion.

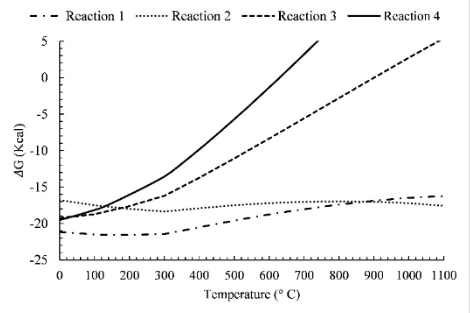

Fig. 1 Gibbs free energy of reaction (1) – (4)

The effect of mixing methods prior decomposition process of ferronickel slag

NaOH addition to the ferronickel slag with ratio 1:1 by weight followed by roasting process assured the transformation of chemical composition, phase, and microstructure. Due to the different mixing methods, physical mixing and impregnation, were performed in this study, the effect of mixing methods that was conducted prior decomposition process to the decomposed ferronickel slag is discussed here.

The transformation of chemical compositions

The chemical compositions of ferronickel slag, RWI, and RI are shown in **Table 1.** It identified MgO and SiO_2 as the main components of ferronickel slag followed by Fe_2O_3, Al_2O_3, and Cr_2O_3. Meanwhile, the remaining components are less than 1 %. Moreover, the chemical compositions of the RWI and RI show that the main components, MgO and SiO_2, experienced significant change by NaOH addition that caused Na_2O composition presented in the roasted products, RWI and RI, at 63.22 and 46.91 %, respectively. It is interesting to note that, the smaller Na_2O content, the higher content of MgO and SiO_2 emerged in the roasted products. The MgO content of RI was higher, about three times, than RWI and exhibited 11.79 %. Meanwhile, the SiO_2 content of RI surpassed RWI one and a half times at 25.16 %. In addition, Al_2O_3 content of RI was higher about 2.5 times than RWI. It indicates that mixing by impregnation that contacted NaOH solution to the surface of ferronickel slag was able to make a better contact and diffusion due to solid-liquid mixing. Therefore, RI resulted in better decomposition compared to RWI that has solid-solid mixing and causing spotted contact that further could form agglomeration to the mixture. However, the content of Fe_2O_3 of raw ferronickel slag, RWI, and RI are exhibited identic for its chemical composition since it used same basis and were calculated as Fe_2O_3 in the XRF analysis. The transformation of phases more affects iron oxide instead of chemical composition in the decomposition process of ferronickel using NaOH.

Table 1 XRF analysis of Ferronickel slag, RWI and RI

Compound (%)	Ferro-nickel slag	RWI	RI
Na_2O	-	63.22	46.91
Al_2O_3	4.04	1.08	2.69
MgO	41.04	3.97	11.79
TiO_2	0.0975	0.108	0.108
Fe_2O_3	10.78	11.37	10.22
SiO_2	40.74	16.89	25.16
CaO	0.7050	0.588	0.607
Cr_2O_3	1.47	1.406	1.289
NiO	0.0535	0.066	0.054
ZnO	0.0255	0.034	0.027

The phase transformations

Fig. 2 describes XRD analysis of ferronickel slag and shows olivine ($(Mg, Fe)_2SiO_4$) as the main phase of ferronickel slag that has a good agreement with the previous research [18], [26] [28].

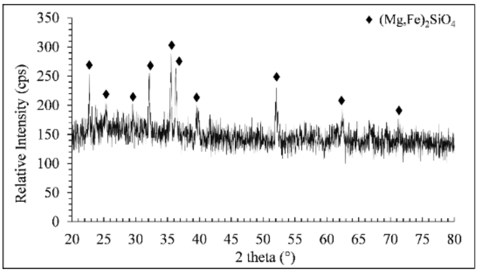

Fig. 2 XRD analysis of ferronickel slag

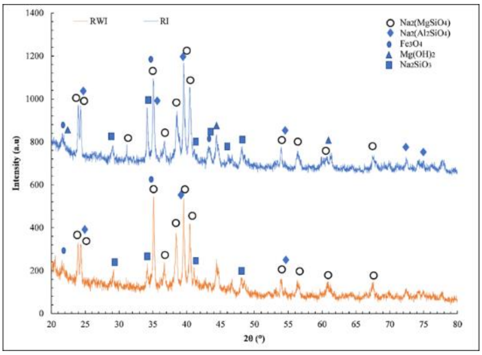

Fig. 3 XRD analysis of RWI and RI

Fig. 3 shows the XRD analysis of the RWI and the RI. $Na_2(MgSiO_4)$, Fe_3O_4, Na_2SiO_3 and $Na_2A_2lSiO_4$ are identified in the RWI and RI, while $Mg(OH)_2$ is just detected in the RI. The existence of $Na_2(MgSiO_4)$ indicates that contact occurred, even though, a longer reaction time might be required to optimize the decomposition process. The presence of Na_2SiO_3 and $Mg(OH)_2$ are in good agreement with the thermodynamic analysis previously. However, $Mg(OH)_2$ was not formed in the RWI. It shows that magnesium silicates, Mg_2SiO_4 and $MgSiO_3$, were not decomposed as reaction **(3)** and **(4)** for RWI and causing higher peak intensity of $Na_2(MgSiO_4)$ at 2θ angle of 35.26 than RI. On the other hand, $Mg(OH)_2$ was detected in the RI and indicates that reaction **(3)** and **(4)** for RI were occurred, causing higher peak intensity of Na_2SiO_3 than RWI especially that is shown on 2θ angle of 34.36 °. The presence of Fe_3O_4 instead of FeO as predicted in the thermodynamic analysis is due to oxidation that might have occurred along the roasting process. Moreover, $Na_2Al_2SiO_4$ formation occurred due to reaction between Aluminium oxide and sodium silicate that might reduce sodium silicate formation in the roasted products.

The morphology transformations

SEM-micrograph and EDS analysis to the raw ferronickel slag were performed in the previous study [18]. It has rough and various particle sizes with Si and O as the primary elements followed by Mg and Fe. **Fig. 4 (a)** and **(b)** depict the morphology of the RWI and the RI respectively. The differences of these two figures are clearly can be seen, irregular surface decomposition of decomposed slag was depicted on the RWI and more eroded reaction product was observed in the RI. This indicates that decomposition process in the RI, which was solid-liquid mixing, was more effective than in the RWI, which was solid-solid mixing.

Fig. 4 (c) and **(d)** depict the areas for EDS analysis of the RWI and RI respectively in the magnification of 2000x. Brightness areas of the RWI (area 1) and the RI (area 2) show that Mg, Al, and Cr have higher content than the areas that have lowest brightness. Meanwhile, Si and Fe was observed on the lowest brightness areas (area 2 of the RWI and area 1 of the RI).

Table 2 Semi-quantitative element analysis of EDS

Element	RWI (%)		RI (%)	
	Area 1	*Area 2*	*Area 1*	*Area 2*
O	42.28	45.41	37.34	40.81
Na	20.18	22.43	25.89	21.97
Mg	15.09	7.75	7.26	13.24
Al	2.91	2.12	1.98	2.14
Si	12.09	15.55	16.69	13.08
Cr	0.66	0.59	1.00	1.03
Fe	4.73	3.72	7.37	4.76
Cu	1.29	1.26	1.66	1.56
Zn	0.77	1.17	0.83	1.41

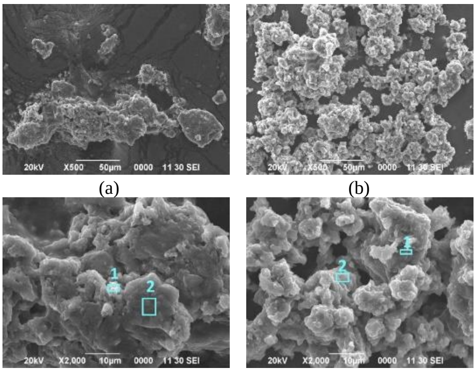

(a) (b)

(c) (d)

Fig. 4 SEM micrograph of (a) RWI with 500x of magnification (b) RI with 500x of magnification (c) RWI with 2000x of magnification (d) RI with 2000x of magnification

Decomposition mechanism of ferronickel slag using NaOH

The mechanism of decomposition process of the RWI and RI are illustrated in **Fig. 5**. Decomposition of the RWI could be occurred after melting point of sodium hydroxide, 318 ˚ C, viscous

DOI: 10.36547/ams.29.4.1925

melted sodium hydroxide could not be dispersed easily and react to the surface that has contact to it, ferronickel slag tends to agglomerate when contact to the viscous melted sodium hydroxide, therefore spotty decomposition occurred, as figure out on **Fig. 5**. Moreover, spotty decomposition is illustrated by SEM-mapping of RWI on **Fig. 6 (a)** and marked by red square in the top-right corner. It shows that Fe and Cr elements clearly distributed on that area without the presence of O, Na, Mg, Al, and Si elements.

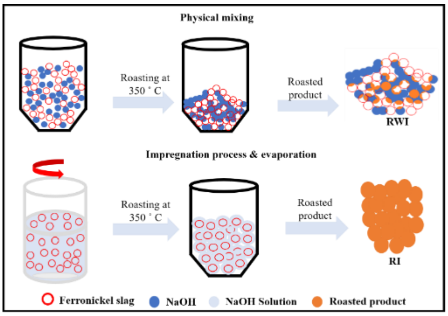

Fig. 5 Mechanism of decomposition process by physical mixing and impregnation

Meanwhile, the larger and further immerse decomposition occurred in the RI as is illustrated in **Fig. 5** and shown in the SEM-mapping of RI in **Fig. 6 (b)**. The elements are uniformly distributed over the surface area. Moreover, Zn content in the RI shows more higher than the RWI. Reaction between sodium hydroxide solution and ferronickel slag allows diffusion occurred from liquid to solid and vice versa. Moreover, the presence of water in the mixture reduced the viscosity of sodium hydroxide solution and increased its flow ability that possibly make larger contact and molecules attachment to the surface of ferronickel slag. Furthermore, it could accelerate breakage of the components especially for Si-O, Mg-O and Al-O [25] that the contents have significantly influenced. Heterogeneous reactions were occurred from surface to the core forming product layer and progressively eroded ferronickel slag as alkali roasting conducted continuously [25]. Therefore, the morphology of RI looked more liberated than RWI.

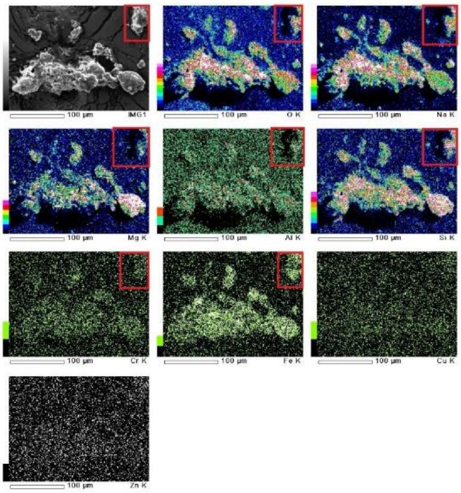

(a)

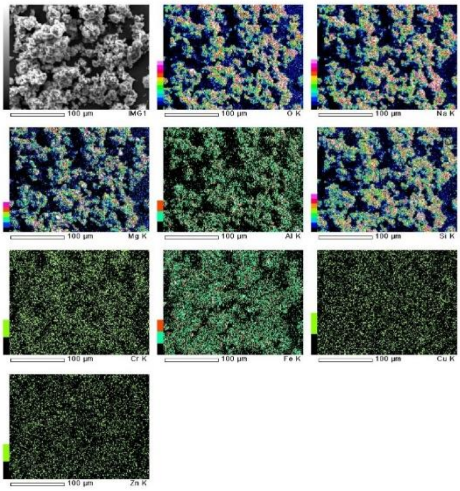

(b)

Fig. 6 SEM-Mapping of **(a)** RWI **(b)** RI

This current work represents how the preliminary process such as mixing process influences interaction between reactants and causing transformation of chemical composition, phases, and microstructure. Mixing by impregnation provides better decomposition compared to physical mixing, especially for sodium silicate formation. Optimization to this process need to be performed in the future to maximized sodium silicate formation and prevent $Na_2Al_2SiO_4$ formation. Therefore, main component of the ferronickel slag, silica, could be selectively extracted first optimally before recovering the other valuable metals.

CONCLUSIONS

The effect of mixing methods prior the decomposition process of ferronickel slag was studied. The effectiveness of impregnation over physical mixing is shown from the characterization results of the decomposed products. XRF analysis shows the higher chemical compositions for Al, Mg and Si by 2.5, 3, and 1.5 times, serially. Moreover, the higher diffraction of sodium silicate phase in the XRD analysis of the RI was also supported. Formation of Na_2SiO_3, $Mg(OH)_2$ and Fe_3O_4 in the XRD analysis indicated that decomposition of ferronickel slag and NaOH was performed and having a good agreement with the thermodynamic analysis. Furthermore, SEM analysis indicates the formation of product layer from reaction of ferronickel slag and NaOH solution of RI are more well distributed, while reaction in the RWI tends to cause spotty decomposition.

Acknowledgments: This work was carried out in The Research Centre for Metallurgy and supported by The Research Programs from Research Organization of Advanced Material, Nanotechnology and Materials, The National Research and Innovation Agency (BRIN), Indonesia, with contract number 3/III.10/HK/2023.

REFERENCES

1. National Minerals Information Center: *Nickel Statistics and Information*. 2017. Accessed: Jun. 20, 2022. [Online]. Available: https://www.usgs.gov/centers/national-minerals-information-center/nickel-statistics-and-information.

2. National Minerals Information Center: *Nickel*. 2022. Accessed: Nov. 28, 2023. [Online]. Available: https://pubs.usgs.gov/periodicals/mcs2023/mcs2023-nickel.pdf.
3. B. Xi, R. Li, X. Zhao, Q. Dang, D. Zhang, W. Tan: Resources, Conservation and Recycling, 139, 2018, 15–16. https://doi.org/10.1016/j.resconrec.2018.08.002
4. A. F. Jiménez, K. Arbi, A. Palomo: Alkali-activated slag cement: Blast furnace versus ferronickel slag, in *34th Cement and Concrete Science Conference*, Sheffield, University of Sheffield, 2014, 203-206.
5. M. A. Rahman, P. K. Sarker, F. Uddin, A. Shaikh, A. K. Saha: Construction and Building Materials, 140, 2017, 194–202. https://doi.org/10.1016/j.conbuildmat.2017.02.023
6. Y. Cheol, S. Choi: Construction and Building Materials, 99, 2015, 279-281. http://dx.doi.org/10.1016/j.conbuildmat.2015.09.039
7. A. K. Saha and P. K. Sarker: Construction and Building Materials, 123, 2016, 135-142. https://doi.org/10.1016/j.conbuildmat.2016.06.144
8. Y. Huang, Q. Wang, and M. Shi: Construction and Building Materials, 156, 2017, 773-789. https://doi.org/10.1016/j.conbuildmat.2017.09.038
9. A. Qi, X. Liu, Z. Wang, and Z. Chen: Construction and Building Materials, 231, 2020, 1-10. https://doi.org/10.1016/j.conbuildmat.2019.117120
10. J. Sun, J. Feng, and Z. Chen: Construction and Building Materials, 206, 2019, 201-209. https://doi.org/10.1016/j.conbuildmat.2019.01.187
11. M. Kimsan, *et.al.*: Key Engineering Materials, 931, 2022, 205-211. https://doi.org/10.4028/p-j30lrv
12. K. Komnitsas, G. Bartzas, V. Karmali, E. Petrakis: Sustainability, 28, 2019, 1 – 16. https://doi.org/10.3390/su11071863
13. J. Yang, X. Duan, L. Liu, H. Yang, and X. Jiang: Minerals, 11(1375), 2021, 1-20. https://doi.org/10.3390/min11121375
14. A. B. Prasetyo *et al.*: Eastern-European Journal of Enterprise Technologies - Materials Science, 12, 2020, 6 – 14. https://doi.org/10.15587/1729-4061.2020.193885
15. A. B. Prasetyo, A. Khaerul, W. Mayangsari, E. Febriana, and A. Maksum: Journal of Mining and Metallurgy Section B- Metallurgy, 57(2), 2021, 225-233. https://doi.org/10.2298/JMMB200224018P
16. Z. Zulhan and N. Agustina: Journal of Cleaner Production, 292, 2021, 1–13. https://doi.org/10.1016/j.jclepro.2020.125307
17. Z. Penga, *et.al.*: Resources, Conservation & Recycling, 149, 2019, 521 – 531. https://doi.org/10.1016/j.resconrec.2019.06.019
18. W. Mayangsari, I. N. Avifah, A. B. Prasetyo, E. Febriana, A. Maksum: Eastern-European Journal of Enterprise Technologies, 2(12), 2021, 44-51. https://doi.org/10.15587/1729-4061.2021.217579
19. Z. Guo, D. Zhu, J. Pan, and F. Zhang: Minerals, 7(98), 2017, 1-16. https://doi.org/10.3390/min7060098
20. A. C. Setyabrata, A. Maksum, A. B. Prasetyo, B. Priyono, J. W. Soedarsono: IOP Conference Series: Materials Science and Engineering, 553, 2019, 1–7. https://doi.org/10.1088/1757-899X/553/1/012028
21. X. Zhang *et al.*: ACS Omega, 4(14), 2019, 16062-16067. https://doi.org/10.1021/acsomega.9b02262
22. J. S. Demotica, R. F. A. Jr, R. M. Malaluan, and C. G. Demayo: International Journal of Environmental Science and Development, 3 (5), 2012, 470–474. https://doi.org/10.7763/IJESD.2012.V3.269
23. F. R. Mufakhir, M. Z. Mubarok, and Z T Ichlas: IOP Conference Series: Materials Science and Engineering, 285, 2018, 1-9. https://doi.org/10.1088/1757-899X/285/1/012003
24. W. Mayangsari *et al.*: Metalurgi, 2, 2021, 43–50. http://dx.doi.org/10.14203/metalurgi.v36i2.588
25. E. Kim, J. Spooren, K. Broos, L. Horckmans, M. Quaghebeur, K. C. Vrancken: Hydrometallurgy, 158(2015), 2020, 139–148. https://doi.org/10.1016/j.hydromet.2015.10.024
26. F. Gu *et al.*: Journal of Hazardous Materials, 374, 2019, 83-91. https://doi.org/10.1016/j.jhazmat.2019.04.002
27. A. B. Prasetyo, A. Maksum, J. W. Soedarsono1, F. Firdiyono: IOP Conf. Series: Materials Science and Engineering, 541, 2019, 1-8. https://doi.org/10.1088/1757-899X/541/1/012037
28. D. Fang, J. Xue, L. Xuan: Recycling SiO_2 and Al_2O_3 from the Laterite Nickel Slag in Molten Sodium Hydroxides, in *9th International Symposium on High-Temperature Metallurgical Processing*, The Minerals, Metals & Materials Series, Switzerland, 2018, 245–257. https://doi.org/10.1007/978-3-319-72138-5_25
29. R. Cao, Z. Jia, Z. Zhang, Y. Zhang, N. Banthia: Cement and Concrete Research, 137, 2020, 1–14. https://doi.org/10.1016/j.cemconres.2020.106202